Generalized Z-Domain Absorbing Boundary Conditions for the Analysis of Electromagnetic Problems With Finite-Difference Time-Domain Method

Zhenhai Shao, Wei Hong, *Member, IEEE*, and Jianyi Zhou

***Abstract*—In this paper, a generalized absorbing boundary condition (Z-ABCs) is constructed in the Z-transform domain. Based on Z-ABCs, some well-known ABCs, such as the Mur's ABC, the dispersive boundary condition, Zhao and Litva's ABC, Liao's ABC, etc. can be easily deduced. Besides, it can also result in some new ABCs. Recurrence formulas for the coefficients of Z-ABCs are presented, and the stability and numerical dispersive characteristics are discussed in detail. In order to validate the Z-ABCs, the finite-difference time-domain method is applied to the analysis of transmission lines, integrated filters, patch antennas, and scattering problems.**

***Index Terms*—Absorbing boundary condition (ABC), electromagnetic, finite-difference time-domain (FDTD) method, numerical dispersive, stability, Z-transform.**

I. Introduction

THE finite-difference time-domain (FDTD) [1] method is a full-wave approach for the analysis of complex electromagnetic problems such as integrated transmission lines, discontinuities, scattering of complex objects and antennas, etc. The vast majority of problems to which the FDTD method is applied involve open structures that require the use of absorbing boundary conditions (ABCs) to correctly terminate the computational domain.

Over the last decades, several kinds of ABCs have been proposed. Generally, there are two ways to construct the ABCs. One is the employment of nonphysical absorbing media, such as the perfect matched layer (PML) [2], which can absorb the wide-angle scattered wave perfectly, but it needs extra computer memory. Another is the usage of outgoing wave equations, such as Mur's ABCs [3], the dispersive boundary conditions (DBCs) [4] and other absorbing conditions presented by Liao *et al.* [5], Lindman [6], Zhao and Litva [7], Zhou and Hong [8], etc. These are substantially simple and do not require extra computer memory.

From [3]–[8], we can find most of those existing outgoing waves' ABCs are constructed in different ways. In this paper, we propose a unified ABC (Z-ABCs) based on the Z-domain transformation. By choosing different polynomic approximations of Z-ABCs, two groups of generalized ABCs and their coefficients can be obtained. Based on the Z-ABCs, some well-known ABCs, such as the Mur's ABC, the DBC, Zhao and Litva's ABC, and Liao's ABC can be easily deduced. Finally, in order to validate our conclusions of the stability and numerical dispersive characteristics and show the efficiency of the Z-ABCs numerically, Z-ABCs combined with the FDTD method are applied to the analysis of transmission lines, integrated filters, patch antennas, and scattering problems.

This paper is organized as follows. In Section II, the Z-ABCs based on the Z-domain transformation are introduced. Recurrence formulas of two groups of Z-ABCs are proposed in Section III. In Section IV, some existing ABCs are obtained from Z-ABCs. The stability and numerical dispersive characteristics of Z-ABCs are given in Sections V and VI, respectively. Finally, some examples are analyzed using Z-ABCs.

II. Unified Z-Transform Domain ABC

In the Z-transform domain, we assume that the scattered wave propagates along the $-x$-direction with the phase velocity v and the truncated boundary is set at $x = 0$. The relationship between the boundary field $E_0(z)$ and interior fields $E_k(z)$, $k = 1, 2, \ldots, p$ is expressed as [8]

$$E_0(z) = \sum_{k=1}^{p} h_k(z) E_k(z) \tag{1}$$

where $h_k(z)$ is the transfer function and p is the order of the ABC.

According to the radiation condition or the transmission condition, E_k, $k = 0, 1, \ldots, p-1$ must satisfy

$$E_k(z) = z^{-s} E_{k+1}(z) \tag{2}$$

where $s = \Delta x / v \Delta t$ and Δx, Δt are the space and time increments, respectively. To absorb the scattered wave with different incident angles in a wide frequency band or propagation wave in a different dielectric layer, which will produce different velocities, p different velocities v_i, $i = 1, 2, \ldots, p$ are considered. According to v_i, $i = 1, 2, \ldots, p$ and $s = \Delta x / v \Delta t$, there is

Manuscript received May 23, 2001; revised May 11, 2002.

Z. Shao is with the State Key Laboratory of Millimeter Waves, Department of Radio Engineering, Southeast University, Nanjing 210096, China and also with the Global Positioning Systems Centre, College of Engineering, Nanyang Technological University, Singapore 639798 (e-mail: ezhshao@ntu.edu.sg).

W. Hong and J. Zhou are with the State Key Laboratory of Millimeter Waves, Department of Radio Engineering, Southeast University, Nanjing 210096, China (e-mail: weihong@seu.edu.cn).

Digital Object Identifier 10.1109/TMTT.2002.806908

a set $\{s_i\}_{i=1}^{p}$. In [8], recurrence formulas for the transfer functions $h_k(z)$ were derived. Here, a more simple and compact expression for the transfer function $h_k(z)$ is derived as

$$h_k = (-1)^{k+1} \sum_{\substack{1\le k_1,\ldots,k_k\le p \\ k_i\neq k_j,\,1\le i,\,j\le k}} (d_{k_1} d_{k_2} \cdots d_{k_k}) \tag{3}$$

where $k = 1, \ldots, p$, $d = z^{-s}$, $d_{k_1} d_{k_2} \cdots d_{k_k}$ is the product of $d_{k_1}, d_{k_2}, \ldots, d_{k_k}$ and s_{k_i} is an element of the set $\{s_i\}_{i=1}^{p}$.

In practice, the phase velocity v is determined by the incidence angle θ of a scattered wave or the effective dielectric constant ε_{eff} of the transmission lines, i.e., $v = v_0/\cos(\theta)$ or $v = v_0/\sqrt{\varepsilon_{\text{eff}}}$, where v_0 denotes the light velocity of free space.

If all factors $s_i = 1$, the transfer function $h_k(z)$ in (3) may be reduced to

$$h_k = (-1)^{k+1} C_k^p z^{-k}, \qquad k = 1, \ldots, p \tag{4}$$

where $C_k^p = p!/((p-k)!k!)$.

By substituting (4) into (1), a special ABC in the Z-transform domain can be obtained as follows:

$$E_0 = \sum_{k=1}^{N} (-1)^{k+1} C_k^N z^{-k} E(x + kv\Delta t). \tag{5}$$

Its inverse Z-transform is just Liao's ABC [5].

Normally, the factor s in the transfer function is not an integer. This means that the time delay of a space increment is not an integer time of the time increment, thus, the transfer function cannot be changed into differential schemes directly. In practical applications, proper simplification is necessary. Two typical approximations are shown in (6) and (7) at the bottom of this page.

By applying (6) and (7) to (3) and (1) and using an inverse Z-transform, two groups of ABCs can be obtained in the time domain.

III. Recurrence Formulas for the Coefficients of the ABCs in Time Domain

In order to use the ABCs of pth-order constructed from (6) or (7), the coefficients of these ABCs must be given. Here, recurrence formulas for the coefficients are derived corresponding to (6) and (7), respectively.

The ABCs of pth order in the time domain constructed from (6) can be expressed as

$$\sum_{j=0}^{p} C_{0,j}^p E_0^{n-j} = \sum_{k=1}^{p} \sum_{j=0}^{p} C_{k,j}^p E_k^{n-j} \tag{8}$$

where E_k^n stands for the field value at the kth node and nth time step $n\Delta t$.

Let

$$a_i = \alpha - (1-\beta)s_i, \qquad i = 1, \ldots, p \tag{9}$$

$$b_i = 1 - (\alpha - (1-\beta)s_i), \qquad i = 1, \ldots, p \tag{10}$$

$$c_i = \alpha + \beta s_i, \qquad i = 1, \ldots, p \tag{11}$$

$$d_i = 1 - (\alpha + \beta s_i), \qquad i = 1, \ldots, p. \tag{12}$$

Recurrence formulas for the coefficients of (8) can then be derived as

$$C_{0,0}^{(1)} = b_1 \tag{13}$$

$$C_{0,1}^{(1)} = a_1 \tag{14}$$

$$C_{1,0}^{(1)} = d_1 \tag{15}$$

$$C_{1,1}^{(1)} = c_1 \tag{16}$$

$$C_{0,0}^{(p)} = C_{0,0}^{(p-1)} b_p \tag{17}$$

$$C_{0,i}^{(p)} = C_{0,i-1}^{(p-1)} a_p + C_{0,i}^{(p-1)} b_p, \qquad i = 1, \ldots, p-1 \tag{18}$$

$$C_{0,p}^{(p)} = C_{0,p-1}^{(p-1)} a_p \tag{19}$$

$$C_{1,0}^{(p)} = C_{0,0}^{(p-1)} d_p + C_{1,0}^{(p-1)} b_p \tag{20}$$

$$C_{1,j}^{(p)} = C_{0,j-1}^{(p-1)} c_p + C_{0,j}^{(p-1)} d_p + C_{1,j-1}^{(p-1)} a_p + C_{1,j}^{(p-1)} b_p, \quad 1 \le j < p \tag{21}$$

$$C_{1,p}^{(p)} = C_{0,p-1}^{(p-1)} c_p + C_{1,p-1}^{(p-1)} a_p \tag{22}$$

$$C_{k,0}^{(p)} = C_{k,0}^{(p-1)} b_p - C_{k-1,0}^{(p-1)} d_p, \qquad k = 2, \ldots, p-1 \tag{23}$$

$$C_{k,j}^{(p)} = C_{k,j-1}^{(p-1)} a_p + C_{k,j}^{(p-1)} b_p - C_{k-1,j-1}^{(p-1)} c_p - C_{k-1,j}^{(p-1)} d_p, \quad 2 \le k < p; \quad 1 < j < p \tag{24}$$

$$C_{k,p}^{(p)} = C_{k,p-1}^{(p-1)} a_p - C_{k-1,p-1}^{(p-1)} c_p, \qquad 2 \le k < p \tag{25}$$

$$C_{p,0}^{(p)} = -C_{p-1,0}^{(p-1)} d_p \tag{26}$$

$$C_{p,i}^{(p)} = -C_{p-1,i-1}^{(p-1)} c_p - C_{p-1,i}^{(p-1)} d_p, \qquad 1 \le i < p \tag{27}$$

$$C_{p,p}^{(p)} = -C_{p-1,p-1}^{(p-1)} c_p. \tag{28}$$

The ABCs of pth order constructed from (7) can be expressed as

$$\sum_{i=0}^{2p} C_{0,i}^p E_0^{n-i} = \sum_{i=1}^{p} \sum_{j=0}^{2p} C_{i,j}^p E_i^{n-j}. \tag{29}$$

$$z^{-s} = \frac{\left(z^{-1}\right)^{\alpha+\beta s}}{\left(z^{-1}\right)^{\alpha-(1-\beta)s}} \approx \frac{1 + (\alpha+\beta s)\left(z^{-1}-1\right)}{1 + \left[\alpha - (1-\beta)s\right]\left(z^{-1}-1\right)} \tag{6}$$

$$z^{-s} = \frac{z^{-\alpha-\beta s}}{z^{-\alpha+(1-\beta)s}} \approx \frac{1 + (\alpha+\beta s)\left(\left(z^{-1}-1\right) + (\alpha+\beta s-1)\left(z^{-1}-1\right)^2/2\right)}{1 + \left[\alpha-(1-\beta)s\right]\left(\left(z^{-1}-1\right) + \dfrac{\left[\alpha-(1-\beta)s-1\right]\left(z^{-1}-1\right)^2}{2}\right)} \tag{7}$$

Let

$$a_i = 1 - (\alpha + \beta s) + (\alpha + \beta s)(\alpha + \beta s - 1)/2 \tag{30}$$

$$b_i = (\alpha + \beta s) - (\alpha + \beta s)(\alpha + \beta s - 1) \tag{31}$$

$$c_i = (\alpha + \beta s)(\alpha + \beta s - 1)/2 \tag{32}$$

$$d_i = 1 - \big[\alpha - (1-\beta)s\big]\left\{1 - \frac{\alpha - (1-\beta)s - 1}{2}\right\} \tag{33}$$

$$e_i = \big[\alpha - (1-\beta)s\big]\Big\{1 - \big[\alpha - (1-\beta)s - 1\big]\Big\} \tag{34}$$

$$f_i = \big[\alpha - (1-\beta)s\big]\big[\alpha - (1-\beta)s - 1\big]/2 \tag{35}$$

where $i = 1, \ldots, p$.

The recurrence formulas for the coefficients $C_{i,j}^{p}$ of (29) can then be derived as

$$C_{0,0}^{1} = d_1 \tag{36}$$

$$C_{0,1}^{1} = e_1 \tag{37}$$

$$C_{0,2}^{1} = f_1 \tag{38}$$

$$C_{1,0}^{1} = a_1 \tag{39}$$

$$C_{1,1}^{1} = b_1 \tag{40}$$

$$C_{1,2}^{1} = c_1 \tag{41}$$

$$C_{0,0}^{(p)} = C_{0,0}^{(p-1)}\, d_p, \qquad p > 1 \tag{42}$$

$$C_{0,i}^{(p)} = C_{0,i-2}^{(p-1)} f_p + C_{0,i-1}^{(p-1)} e_p + C_{0,i}^{(p-1)}\, d_p, \quad i = 1, \ldots, 2p-1,\ p > 1 \tag{43}$$

$$C_{0,2p}^{(p)} = C_{0,2(p-1)}^{(p-1)} f_p \tag{44}$$

$$C_{1,i}^{(p)} = C_{1,i-2}^{(p-1)} f_p + C_{1,i-1}^{(p-1)} e_p + C_{1,i}^{(p-1)}\, d_p + C_{0,i-2}^{(p-1)} c_p + C_{0,i-1}^{(p-1)} b_p + C_{0,i}^{(p-1)} a_p \quad i = 0, \ldots, 2p-1;\quad p > 1 \tag{45}$$

$$C_{1,2p}^{(p)} = C_{1,2(p-1)}^{(p-1)} f_p + C_{0,2(p-1)}^{(p-1)} c_p, \qquad p > 1 \tag{46}$$

$$C_{k,i}^{(p)} = C_{k,i-2}^{(p-1)} f_p + C_{k,i-1}^{(p-1)} e_p + C_{k,i}^{(p-1)} d_p - C_{k-1,i-2}^{(p-1)} c_p - C_{k-1,i-1}^{(p-1)} b_p - C_{k-1,i}^{(p-1)} a_p, \quad k = 2, \ldots, p-1;\quad i = 0, \ldots, 2p-1 \tag{47}$$

$$C_{k,2p}^{(p)} = C_{k,2(p-1)}^{(p-1)} f_p - C_{k-1,2(p-1)}^{(p-1)} c_p, \quad k = 2, \ldots, p-1 \tag{48}$$

$$C_{p,0}^{(p)} = -C_{p-1,0}^{(p-1)} a_p \tag{49}$$

$$C_{p,i}^{(p)} = -C_{p-1,i-2}^{(p-1)} c_p - C_{p-1,i-1}^{(p-1)} b_p - C_{p-1,i}^{(p-1)} a_p \quad i = 1, \ldots, 2p-1 \tag{50}$$

$$C_{p,2p}^{(p)} = -C_{p-1,2(p-1)}^{(p-1)} c_p. \tag{51}$$

Using these two groups of recurrence formulas, the ABCs of pth order constructed from (6) and (7) are then deduced as (8) and (29), respectively.

TABLE I
SOME EXISTING ABCS, WHICH CAN BE DEDUCED FROM (6)

α	β	p	ABCs
0	0	≥ 1	the ABC by Zhao and Litva [7]
0	1	≥ 1	the ABC by Zhou and Hong [8]
0.5	0.5	1	1st order Mur's ABC [3]
0.5	0.5	2	DBC [4]

IV. DERIVATION OF SOME EXISTING ABCS

We can easily deduce some existing ABCs by choosing different parameters α, β, and p in (6) and substituting them into (8). Table I shows some special cases.

V. STABILITY ANALYSIS

It is known that some ABCs are not stable in some special cases. Thus, we must investigate the stability and numeric dispersibility of the ABCs. Here, the stability of the ABCs constructed from (6) is investigated based on the Von Neumann (Fourier series) method.

The first-order ABC constructed from (6) can be written as

$$\big[1 + s - (\alpha + \beta s)\big]E_0^n + \big[(\alpha + \beta s) - s\big]E_0^{n-1} = \big[1 - (\alpha + \beta s)\big]E_1^n + (\alpha + \beta s)E_1^{n-1}. \tag{52}$$

Considering the solution of the following type:

$$E^k(x_i) = V^k(l)e^{j\sigma x_i} \tag{53}$$

where $j = \sqrt{-1}$, $\sigma = 2\pi l$ ($l = \pm 1, \pm 2, \ldots$). Let $V^n/V^{n-1} = G$, then (52) is reduced to

$$G = \frac{s\cos\left(\frac{\sigma\Delta x}{2}\right) + j\big[2(\alpha + \beta s) - s\big]\sin\left(\frac{\sigma\Delta x}{2}\right)}{s\cos\left(\frac{\sigma\Delta x}{2}\right) - j\Big\{2\big[1 - (\alpha + \beta s)\big] + s\Big\}\sin\left(\frac{\sigma\Delta x}{2}\right)} \tag{54}$$

and

$$|G|^2 = \frac{s^2 + \big[4(\alpha+\beta s)^2 - 4(\alpha+\beta s)s\big]\sin^2\left(\frac{\sigma\Delta x}{2}\right)}{s^2 + \big[4(\alpha+\beta s)^2 + 4 + 4s - (\alpha+\beta s)(8+4s)\big]\sin^2\left(\frac{\sigma\Delta x}{2}\right)}. \tag{55}$$

If the difference scheme of (52) is stable, there must exist c and s_0 such that the following inequation is valid:

$$|G(\sigma, s)| < 1 + cs, \qquad 0 < s < s_0. \tag{56}$$

For (52), therefore, the following unconditional stable condition is derived:

$$\alpha + \beta s < (1 + s)/2 \tag{57}$$

and the conditional stable condition is derived as follows:

$$\alpha + \beta s = (1 + s)/2. \tag{58}$$

It must be pointed out that unconditional stability occurs when condition (57) is chosen, the ABC (52) is always stable

without other conditions; condition stable denotes that, although (58) is satisfied, the ABC (52) may diverge in some special conditions.

As shown in Section IV, the ABCs presented by Mur [3], Zhao and Litva [7], Zhou and Hong [8], and the DBC [4], etc. can be deduced from (6); thus, the conclusions above are valid for these well-known ABCs.

It can be shown that the stability conditions of (57) and (58) can also ensure the stability of the higher order ABCs derived from (6).

Since the ABCs derived from (7) are a higher approximation than the ABCs derived from (6), conditions (57) and (58) can also ensure the stability of ABCs derived from (7) according to the following detailed examples.

VI. Numeric Dispersive Characteristic Analysis

When a Gaussian pulse travels on a microstrip-like transmission line, the velocities of fields are different for different frequencies due to the dispersion property. Here, we will analyze the numeric dispersion property of ABC (52).

In three-dimensional (3-D) space, a homochromous plane wave can be written as

$$E^n(I,\,J,\,K) = E_0 e^{j(k_x I\Delta x - k_y J\Delta y - k_z K\Delta z + \omega n\Delta t)}. \quad (59)$$

Rewriting (52) as

$$\begin{aligned}\Big\{1-\big[\alpha-(1-\beta)s\big]\Big\}&E^n(I=0,\,J,\,K)\\ &+\big[\alpha-(1-\beta)s\big]E^{n-1}(I=0,\,J,\,K)\\ =\big[1-(\alpha+\beta s)\big]&E^n(I+1=1,\,J,\,K)\\ &+(\alpha+\beta s)E^{n-1}(I+1=1,\,J,\,K)\end{aligned} \quad (60)$$

and substituting (59) into (60) yields

$$\begin{aligned}e^{j\omega\Delta t/2}\sin(k_x\Delta x/2) - se^{-jk_x\Delta x/2}\sin(\omega\Delta t/2)\\ -2j(\alpha+\beta s)\sin(\omega\Delta t/2)\sin(k_x\Delta x/2)=0.\end{aligned} \quad (61)$$

Dividing (61) into a real part and imaginary part, the following two equations can be derived:

$$\cos\left(\frac{\omega\,\Delta t}{2}\right)\sin\left(\frac{k_x\Delta x}{2}\right) - s\cos\left(\frac{k_x\Delta x}{2}\right)\sin\left(\frac{\omega\,\Delta t}{2}\right)=0 \quad (62)$$

and

$$\sin(\omega\Delta t/2)\sin(k_x\Delta x/2)\big[1+s-2(\alpha+\beta s)\big]=0. \quad (63)$$

If

$$s=\Delta x/(v\Delta t)=1 \quad (64)$$

then (62) can be rewritten as

$$\sin(w\Delta t/2 - k_x\Delta x/2)=0. \quad (65)$$

Hence,

$$w=k_x v. \quad (66)$$

Since the perfect dispersive condition is

$$w^2/v^2 = k_x^2+k_y^2+k_z^2 \quad (67)$$

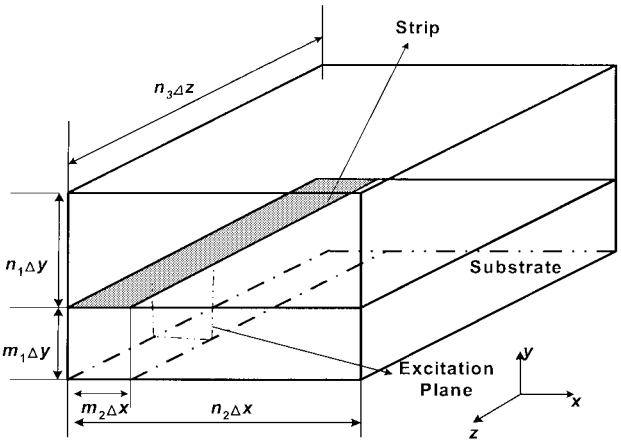

Fig. 1. Structure of a microstrip.

there is no numeric dispersion in x-direction as $s = \Delta x/(v\Delta t) = 1$.

In our 3-D FDTD method, we always let $\Delta x/(v_0\Delta t)=2$. In scattering problems, since $v = v_0/\cos(\theta)$, $\theta = 60^\circ$ is satisfied with a numeric dispersion condition and, in microstrip problems, since $v = v_0/\sqrt{\varepsilon_{\text{eff}}}$ and $\varepsilon_{\text{eff}} > 1$, it is not possible to satisfy numeric dispersion conditions.

From (63), the following relation can be obtained:

$$\alpha+\beta s=(1+s)/2. \quad (68)$$

Thus, when α and β satisfy condition (68), numeric dispersion of Z-ABCs (8) is minimum. However, condition (68) is conditional stable, so it cannot be said that condition (68) is stable and has minimum numeric dispersion.

Since the ABCs derived from (7) are a higher approximation than the ABCs derived from (6), the dispersive condition of ABCs derived from (6) can also be applied to ABCs derived from (7) according to the following detailed examples.

VII. Applications

In order to assess their efficiency, Z-ABCs (8) and (29) are applied to the analysis of microstrip transmission lines, low-pass and bandpass filters, patch antennas, and scattering problems. In the following examples, all metals are perfect conductors.

A. Microstrip Transmission Lines

As shown in Fig. 1, the thickness and dielectric constant of the microstrip substrate are 0.1 and 13 mm, respectively, the width of the metal strip is 0.15 mm, the mesh spaces are $\Delta x = \Delta y = \Delta z = \Delta h = 0.0125$ mm, and the number of nodes (see Fig. 1) are $n_1 = 11$, $n_2 = 40$, $m_1 = 8$, $m_2 = 6$, and $n_3 = 119$. Here, only half of the structure is considered due to the symmetry. The microstrip is excited by a Gaussian pulse at the center of the cross section under the strip and only the E_y component is assumed as

$$E_y^i = \exp\left[-(t-t_0)^2/T^2\right] \quad (69)$$

where $t_0 = 164\Delta t$ and $T = 42\Delta t$. Along the z-direction, the incidence port is 20 meshes away from the front truncation, and the reference port is 40 meshes away from the front truncation.

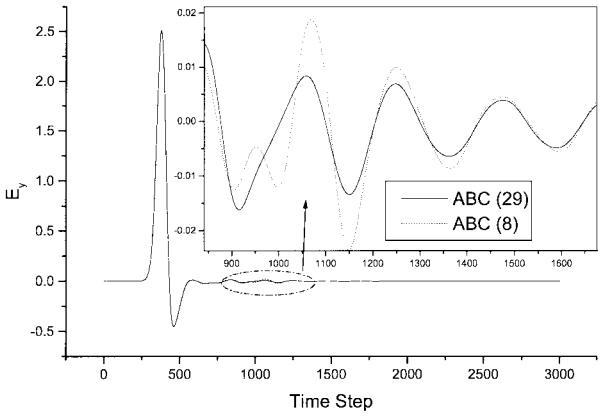

Fig. 2. Comparison of the vertical electric fields with respect to ABCs (8) and (29), where $\alpha = 0.25$ and $\beta = 0.25$.

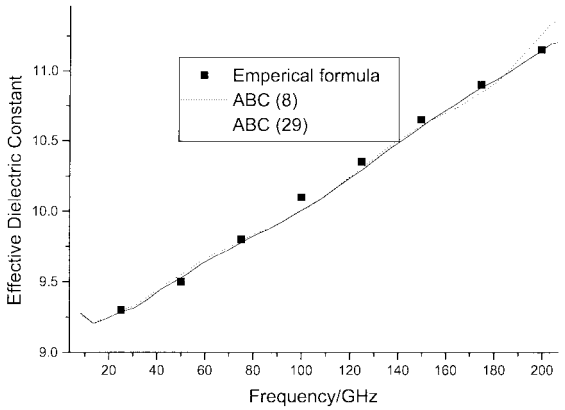

Fig. 3. Comparison of the effective dielectric constants with respect to ABCs (8) and (29), where $\alpha = 0.25$ and $\beta = 0.25$.

Along the z-direction, ABC (8) or (29) of the second order are used, in which $v_1 = v_0/\sqrt{9}$, $v_2 = v_0/\sqrt{11}$. Along the x- and y-directions, ABC (8) or (29) of the first order are used, in which $v = v_0/\sqrt{9.12}/\cos\theta$, where $\theta = 30°$ or $0°$, corresponding to the x- or y-direction, respectively, where 9, 11, and 9.12 are the experiential effective dielectric constant. Normally, they are chosen in the neighbor of the effective dielectric constant of central work frequency. The vertical electric field at the central point under the strip in the excitation plane is sampled.

The vertical electric field and effective dielectric constant are shown in Figs. 2 and 3, respectively. It can be seen that the vertical electric field reflected from boundaries using ABC (29) is reduced over 30% compared with the results using ABC (8), and the effective dielectric constant with respect to ABC (29) is better than that by using ABC (8). The reflection reduction rates for different parameters α, β are shown in Table II.

Fig. 4 shows the vertical electric field with ABC (8) and $\alpha = 0.15$ and $\beta = 0.85$. It can be seen that the field diverges. In fact, if $\alpha = 0.15$ and $\beta = 0.85$, they do not satisfy conditions (57) and (58). In other words, conditions (57) and (58) theoretically are numerically verified to be true.

B. Low-Pass and Bandpass Filters

A microstrip low-pass filter is shown in Fig. 5. The mesh spaces used here are $\Delta x = 0.4064$ mm, $\Delta y = 0.265$ mm,

TABLE II
REFLECTION REDUCTION RATE OF FIELD E_y USING ABC (29) COMPARED WITH THAT USING ABC (8) CORRESPONDING TO DIFFERENT PARAMETERS α, β

α	β	Reflection Reduction Rate
0.5	0.5	10%-17%
0.25	0.25	15%~55%
1	0	34%~56%
0.75	0.25	15%~35%
0	0	40%~60%

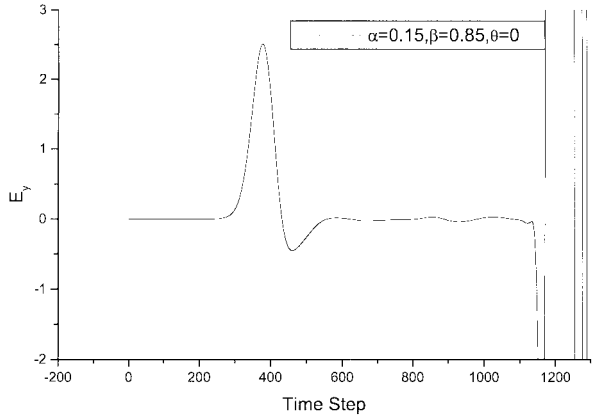

Fig. 4. Vertical electric field at the center of the excitation plane under the strip with ABC (8) for $\alpha = 0.15$ and $\beta = 0.85$.

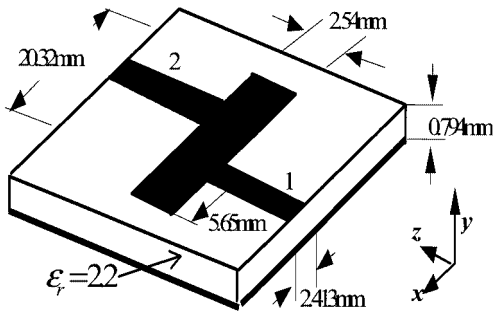

Fig. 5. Configuration of a microstrip low-pass filter.

and $\Delta z = 0.4233$ mm, and the total number of nodes is $80 \times 16 \times 130$. The meshes on the long rectangular patch are $50\Delta x \times 6\Delta z$. The distance from the excitation plane to the edge of the long patch is $50\Delta z$, and both reference planes 1 and 2 are $10\Delta z$ away from the edges of the patch. The strip widths of ports 1 and 2 are assumed as $6\Delta x$. Along the z-direction, ABC (29) of the second order is used, in which $v_1 = v_0/\sqrt{1.7}$ and $v_2 = v_0/\sqrt{2.2}$. Along x- and y-directions, ABC (29) of the first order is used, in which $v = v_0/\sqrt{1.89}/\cos\theta$ and θ is 30° and 0°, corresponding to x- and y-directions, respectively. The scattering parameters are shown in Fig. 6. They are in good agreement with the reported and experimental results.

A microstrip bandpass filter is shown in Fig. 7 and the computed scattering parameters are shown in Fig. 8 with ABC (29). Along the z-direction, ABC (29) of the second order is used, in which $v_1 = v_0/\sqrt{6.6}$ and $v_2 = v_0/\sqrt{9.5}$. Along the x- and y-directions, ABC (29) of the first order is used, in which

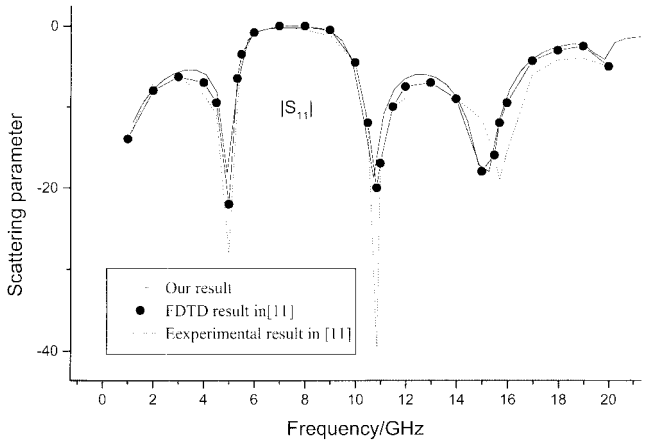

(a)

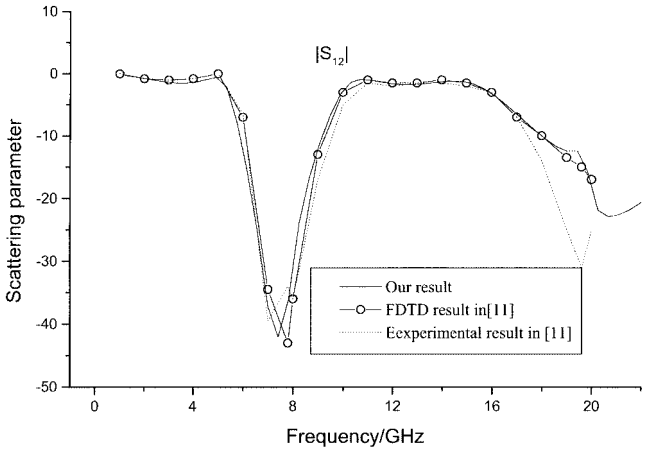

(b)

Fig. 6. Scattering parameters of the low-pass filter.

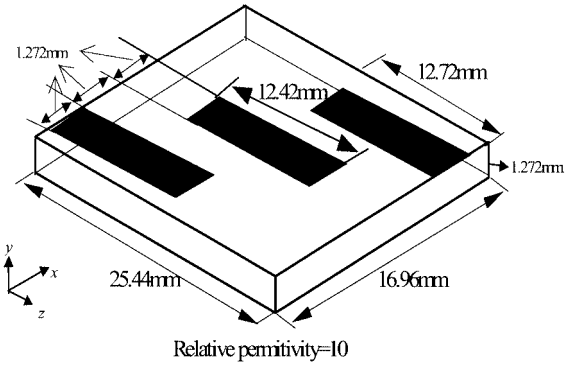

Fig. 7. Configuration of a microstrip bandpass filter.

$v = v_0/\sqrt{6.85}/\cos\theta$ and θ is 30° and 0°, corresponding to the x- and y-directions, respectively. The results are in agreement with the results reported in [11]. For this filter, a uniform mesh space $\Delta x = \Delta y = \Delta z = 0.318$ mm is used.

C. Patch Antenna

A microstrip patch antenna printed on a Duroid ($\varepsilon_r = 2.2$) dielectric substrate is shown in Fig. 9. The mesh spaces used here are $\Delta x = 0.389$ mm, $\Delta y = 0.265$ mm, and $\Delta z = 0.4$ mm, and the total number of nodes is $74 \times 16 \times 140$. Along the z-direction, ABCs (8) or (29) of the second order are used, in

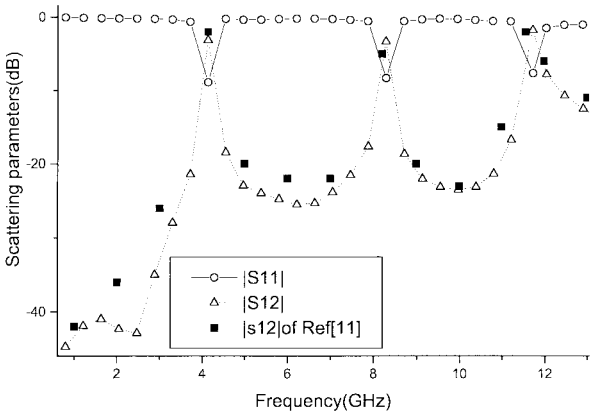

Fig. 8. Scattering parameters of the bandpass filter.

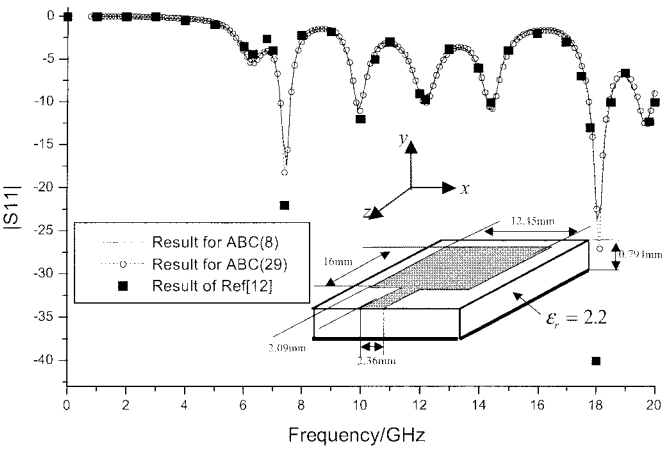

Fig. 9. Return-loss of a microstrip patch antenna.

which $v_1 = v_0/\sqrt{1.8}$ and $v_2 = v_0/\sqrt{2.2}$. Along the x- and y-directions, ABC (8) or (29) of the first order are used, in which $v = v_0/\sqrt{1.88}/\cos\theta$, where $\theta = 30°$ or 0°, corresponding to the x- or y-direction, respectively. For $\alpha = \beta = 0.25$, the return loss corresponding to ABC (8) and ABC (29) is shown in Fig. 9, which is in good agreement with [12].

D. Scattering Problem

Fig. 10 illustrates the geometry of a cube scattering problem. The electrical size of the cube is assumed to be $k_0 s = 2$, where s is the side width of the cube. The Gauss pulse excitation is supposed as

$$E_z^i = \exp\left[-\left(t - t_0 - (z - z_0)/v\right)^2/T^2\right] \qquad (70)$$

and propagates along the y-direction. For the FDTD analysis, the cube is embedded in a $50 \times 50 \times 50$ spatial cell lattice, and each side of the cube is spanned by 400 square cells (20×20).

Fig. 11 shows the comparison of the magnitude and phase of the current along the path $ab'c'd$ with $\theta = 0°$ and different parameters α, β in ABC (8) of the first order. In Fig. 11(a), the current magnitude with $\alpha = -1$, $\beta = -1$ in ABC (8) of the first order agrees with the method of moments (MoM) solution better than other parameters. As $\alpha + \beta s$ increases, the current magnitude error with ABC (8) of the first order also increases. In Fig. 11(b), however, the current phase with $\alpha = 0$, $\beta = 1$ in

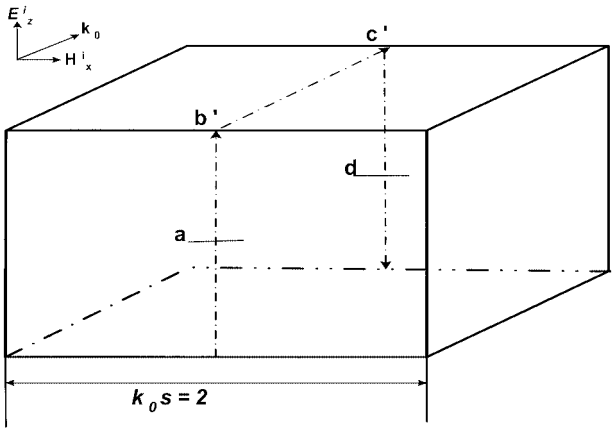

Fig. 10. Geometry of metal-cube scatterer.

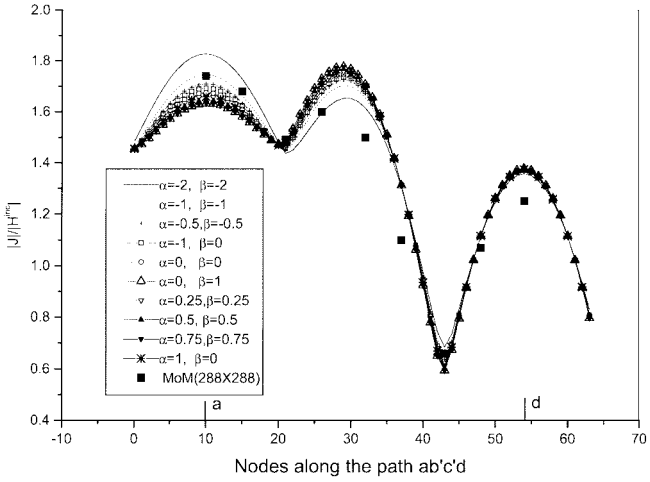

(a)

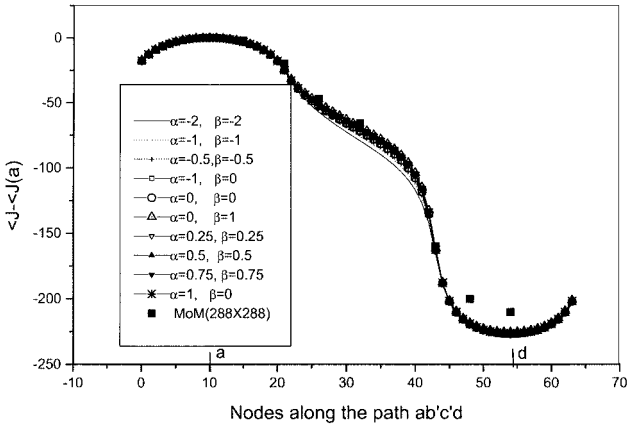

(b)

Fig. 11. Current magnitude and phase with different parameters.

ABC (8) of the first order agrees with the MoM solution better than with other parameters. As $\alpha+\beta s$ decreases, the phase error of the current with ABC (8) of the first order increases. In most cases, therefore, the suitable parameters α, β with ABC (8) of the first order should be chosen in $-1-s \le \alpha+\beta s \le s$.

Fig. 12 shows the magnitude and phase of the current with different angles θ in ABC (8) of the first order, where $v = v_0/\cos(\theta)$ and the angle is the same for all the absorbing boundaries. In Fig. 12(a), the current magnitude for $\theta = 30°$ agrees with the MoM solution better than the others along $\overline{ab'}$. The current magnitude for $\theta = 60°$ agrees with the MoM solution better than the others along $\overline{b'c'}$, and the current magnitude for $\theta = 0°$ agrees with the MoM solution better than the others along $\overline{c'd}$. In Fig. 12(b), however, the current phase for $\theta = 30°$ agrees with the MoM solution better than the others along $\overline{ab'c'}$, and the current phase for $\theta = 0°$ agrees with the MoM solution better than the others along $\overline{c'd}$. Therefore, it is difficult to choose a perfect angle with respect to such scattering problems if we use ABC (8) of the first order. Normally, we may choose an angle between 15°–45°.

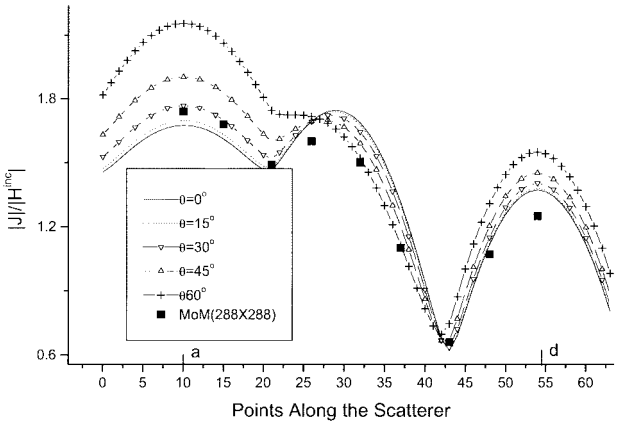

(a)

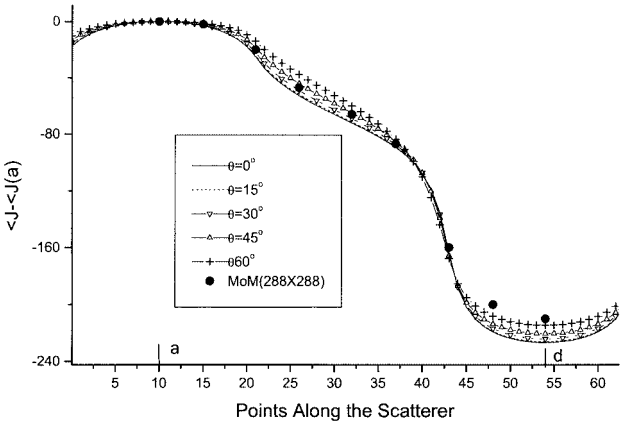

(b)

Fig. 12. Current magnitude and phase with different angles in ABC (8) of the first order.

Fig. 13 shows the current magnitude with ABC (8) of the first, second, and third orders, respectively, where $\alpha = \beta = 0$. The angle with ABC (8) of the first order in all directions is 0°. Two groups of ABCs of the second order are considered. The angles of the first group are 0° and 15° in all directions, and those of the second group are 0° and 15° in the z-direction and 30° and 45° in x- and y-directions, respectively. The angles in ABC (8) of the third order are 0°, 15°, and 30°. In Fig. 13, the current magnitude obtained by ABC (8) of the second order agrees with that by ABC (8) of the third order. Obviously, the results with ABC (8) of the first order are worse than those of the second and third orders. Normally, in scattering problems, ABC (8) of the second order is suitable.

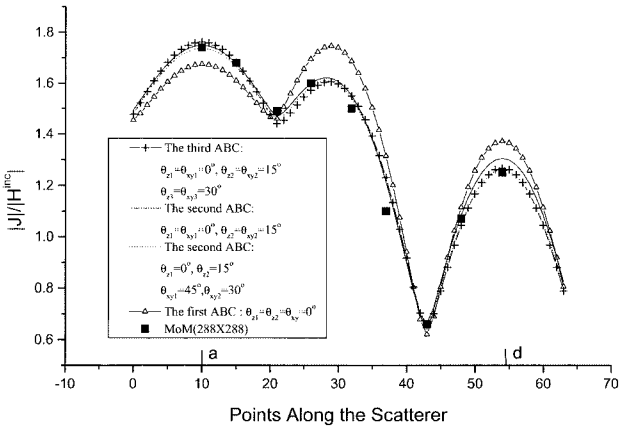

Fig. 13. Current magnitude with ABC (8) of the first, second, and third orders.

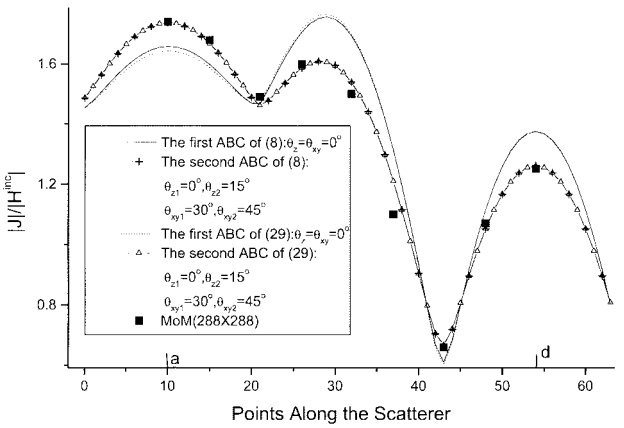

(a)

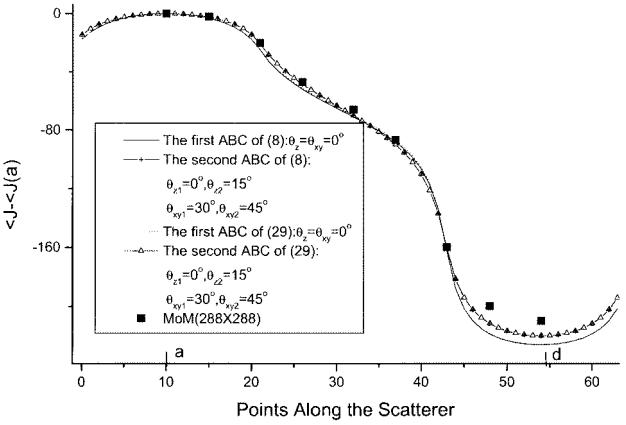

(b)

Fig. 14. Current magnitude and phase with different ABCs (8) and (29) of different orders.

Fig. 14 illustrates the current magnitude and phase with ABCs (8) and (29), where $\alpha = 1$ and $\beta = 0$. As shown in Fig. 14(a), the current magnitude obtained by using ABC (29) of the second order is better than that obtained by using ABC (8) of the second order by approximately 1%. The phase obtained by using ABC (29) of the second order is better than those by using ABC (8) of the second order by 5%$\sim$10% [see Fig. 14(b)]. Usually, this difference between ABC (8) and ABC (29) is not very obvious in scattering problems, but ABC (29) needs more memory. For scattering problems, therefore, ABC (8) is more usable than ABC (29).

With the same parameters α, β and the angle θ, the conclusions resulting from ABC (8) are also valid for ABC (29).

In this section, Z-ABCs have been used to analyze the microstrip line, filter, patch antenna, and scattering problems. From these results, we find that a better result can be obtained by using Z-ABCs of the second order in all kinds of problems. In order to get good results, the stability condition of (57) must be satisfied. According to our experience, when $0 < \alpha, \beta \leq 1/2$, better results can be obtained. Considering the computer memory and calculated time, for propagate problems, Z-ABCs (29) is the optimal choice, and Z-ABCs (8) is a better choice for scattering problems. In order to get better results, in propagate problems, different pre-estimated ε_{eff} can be chosen by a quasi-static expression in the range of the working frequency. According to our experience, ε_{eff} can be chosen between the average of all dielectric constants and the maximum value of all dielectric constants; in scattering problems, in every direction, different angles θ can be chosen between the minimum incident angle and the maximum incident angle, where the incident angle is the angle from the center point of the incident face in that direction to the scattering object. If we do not consider the affection of corners and edges, the Z-ABCs of the third and higher orders will have bigger reflections than those of the second order.

VIII. Conclusions

In this paper, two groups of generalized ABCs are derived in the Z-transform domain, and their stability and numerical dispersive characteristics are discussed. Compared with many existing outgoing wave's ABCs, such as DBC, the coefficient of higher order Z-ABCs can be more easily obtained by recurrence formulas. Z-ABCs of the second order only need two-thirds of the meshes of Z-ABCs of the first order. Since both tangential electric fields and normal magnetic field are absorbed by Z-ABCs in our method, the affection of corners and edges is ignored. This is the main reason why Z-ABCs of the third and higher orders have bigger reflections than Z-ABCs of the second order. By choosing $0 < \alpha, \beta \leq 1/2$ and other suitable parameters, Z-ABCs can always get stable and good results. Compared with the PML condition, although they need more meshes away from discontinuous points, Z-ABCs do not need many absorbing layers and do not need to divide field elements and calculate complex Maxwell equations. Importantly, the traditional PML can only absorb dielectric radiation and has much difficulty in dealing with conducting structures. However, Z-ABCs can deal with any electromagnetic structures. Of course, Z-ABCs have some limitations in connection with high-order FDTD methods.

Acknowledgment

The authors would like to thank N. Murphy, Nanyang Technological University of Singapore, Singapore, and the reviewers for their helpful suggestions and comments.

REFERENCES

[1] K. S. Yee, "Numerical solution for initial boundary value problems involving Maxwell's equation in isotropic media," *IEEE Trans. Antennas Propagat.*, vol. 14, pp. 302–307, May 1996.

[2] J. P. Berenger, "A perfectly matched layer for the absorption of electromagnetic wave," *J. Comput. Phys.*, pp. 185–200, Oct. 1994.

[3] G. Mur, "Absorbing boundary conditions for the finite-difference approximation of the time-domain electromagnetic field equations," *IEEE Trans. Electromagn. Compat.*, vol. EMC-23, pp. 377–382, Nov. 1981.

[4] C. J. Railton, E. M. Daniel, D. L. Paul, and J. P. McGreehan, "Optimized absorbing boundary conditions for the analysis of planar circuits using the finite difference time domain method," *IEEE Trans. Microwave Theory Tech.*, vol. 41, pp. 192–203, Feb. 1993.

[5] Z. P. Liao, H. L. Wong, B. P. Yang, and Y. F. Yuan, "A transmitting boundary for transient wave analysis," *Scientia*, ser. A, vol. 27, no. 10, pp. 1063–1076, 1984.

[6] E. L. Lindman, "Free space boundary conditions for the time dependent wave equation," *J. Comput. Phys.*, vol. 18, pp. 66–78, 1975.

[7] P. Zhao and J. Litva, "A new stable and very dispersive boundary condition for the FDTD method," in *IEEE MTT-S Int. Microwave Symp. Dig.*, 1994, pp. 35–38.

[8] J. Y. Zhou and W. Hong, "Construction of the absorbing boundary conditions for the FDTD method with transfer Functions," *IEEE Trans. Microwave Theory Tech.*, vol. 46, pp. 1807–1809, Nov. 1998.

[9] A. Taflove and K. Umashankar, "Radar cross section of general three-dimensional scatterers," *IEEE Trans. Electromagn. Compat.*, vol. EMC-25, pp. 433–440, Nov. 1983.

[10] D. M. Sheen, S. M. Ali, M. D. Abouzahra, and J. A. Kong, "Application of the three dimensional finite-difference time-domain method to the analysis of planar microstrip circuits," *IEEE Trans. Microwave Theory Tech.*, vol. 38, pp. 849–857, July 1990.

[11] J. Chen, C. Wu, K. Y. Lo, K. L. Wu, and J. Litva, "Using linear and nonlinear predictors to improve the computational efficiency of the FD-TD algorithm," *IEEE Trans. Microwave Theory Tech.*, vol. 42, pp. 1992–1997, Oct. 1994.

[12] G. Kondylis, G. Pottie, and F. D. Flaviis, "Generalized reduced FDTD formulation (R-FDTD) for the solution of Maxwell equations," in *Asia–Pacific Microwave Conf.*, vol. 1, Yokohama, Japan, Dec. 8–11, 1998, pp. 187–190.

Zhenhai Shao was born in Jiangsu, China, on December 1, 1971. He graduated from the Nanjing Normal University of China, Nanjing, China, in 1994. He received the M.S. and Ph.D. degrees from the Southeast University of China, Najing, China, in 1997 and 2000, respectively.

From 2000 to 2001, he was with the National University of Singapore. He is currently a Research Fellow with the Department of Electric and Electronic Engineering, Nanyang Technological University of Singapore. He has authored approximately 20 technical publications. His research interests include the design and simulation of package of monolithic microwave integrated circuit (MMIC) and planar microwave circuits, numerical procedures of FDTD, transmission-line matrix (TLM), time-domain finite-element method (TDFEM), and discrete singular convolution (DSC) method for passive microwave components and software design.

Wei Hong (M'92) was born in Hebei Province, China, on October 24, 1962. He received the B.S. degree from the Zhenzhou Institute of Technology, Zhenzhou, China, in 1982, and the M.S. and Ph.D. degrees from Southeast University, Nanjing, China, in 1985 and 1988, respectively, all in radio engineering.

Since 1988, he has been with the State Key Laboratory of Millimeter Waves, Southeast University, where he is currently a Professor and the Associate Dean of the Department of Radio Engineering. In 1993 and 1995–1998, he was a short-term Visiting Scholar with the University of California at Berkeley and the University of California at Santa Cruz. He has authored and coauthored over 200 technical publications and also authored *Principle and Application of the Method of Lines* (Nanjing, China: Southeast Univ. Press, 1993). He served as a reviewer for many technical journals, including the *Proceedings of the Institution of Electrical Engineers, Part H, Electronics Letters*, etc. He has been engaged in numerical methods for electromagnetic (EM) problems, millimeter-wave theory and technology, antennas, EM scattering, inverse scattering and propagation, RF front-ends for mobile communications, the parameters extraction of interconnects in very large scale integration (VLSI) circuits, etc.

Prof. Hong is a Senior Member of the China Institute of Electronics (CIE). He served as the reviewer for many technical journals, including the IEEE TRANSACTIONS ON MICROWAVE THEORY AND TECHNIQUES and the IEEE TRANSACTIONS ON ANTENNAS AND PROPAGATON. He was the two-time recipient of the First-Class Science and Technology Progress Prizes presented by the State Education Commission in 1992 and 1994, respectively. He was the recipient of the 1991 Fourth-Class National Natural Science Prize and the Third-Class Science and Technology Progress Prize of Jiangsu Province. He was also the recipient of the Trans-Century Training Programme Foundation for the Talents presented by the State Education Commission, the Foundation for China Distinguished Young Investigators presented by the National Science Foundation (NSF), China, the Distinguished China Doctorate Recipients presented by the State Education Commission, and the JiangSu Young Scientist Award presented by the JiangSu Province Government.

Jianyi Zhou was born in JiangSu Province, China, in June 1971. He received the B.S., M.S., and Ph.D. degrees from Southeast University, Nanjing, China, in 1993, 1996, and 2001, respectively, all in radio engineering.

Since 1996, he has been with the State Key Laboratory of Millimeter Waves, Southeast University, where he is currently an Associate Professor. He has authored over 20 technical publications. He has been engaged in numerical methods for electromagnetic problems, RF front-ends for mobile communications, etc.